



HAL
open science

RFID tracking for monitoring deadwood mobility in a small coastal Mediterranean mountainous river: implementation and preliminary results

François Charles, Lucas Laveissière, Michel Groc, Jean-André Magdalou,
Joseph Garrigue

► To cite this version:

François Charles, Lucas Laveissière, Michel Groc, Jean-André Magdalou, Joseph Garrigue. RFID tracking for monitoring deadwood mobility in a small coastal Mediterranean mountainous river: implementation and preliminary results. 2024. hal-04443320

HAL Id: hal-04443320

<https://hal.science/hal-04443320>

Preprint submitted on 7 Feb 2024

HAL is a multi-disciplinary open access archive for the deposit and dissemination of scientific research documents, whether they are published or not. The documents may come from teaching and research institutions in France or abroad, or from public or private research centers.

L'archive ouverte pluridisciplinaire **HAL**, est destinée au dépôt et à la diffusion de documents scientifiques de niveau recherche, publiés ou non, émanant des établissements d'enseignement et de recherche français ou étrangers, des laboratoires publics ou privés.

1 Ce manuscrit est destiné au numéro spécial "50 ans de la Massane"

2 Titre

3 RFID TRACKING FOR MONITORING DEADWOOD MOBILITY IN A SMALL COASTAL MEDITERRANEAN
4 MOUNTAINOUS RIVER: IMPLEMENTATION AND PRELIMINARY RESULTS

5

6 Noms des auteurs en italique et en majuscules ;

7 *FRANÇOIS CHARLES*(a), LUCAS LAVEISSIERE(b), MICHEL GROC(b), JEAN-ANDRE MAGDALOU(c), JOSEPH*
8 *GARRIGUE(c)*

9

10 Affiliations et adresses des auteurs, y compris l'adresse électronique de l'auteur correspondant ;

11 (a) Sorbonne Université, CNRS, UMR8222, Laboratoire d'Ecogéochimie des Environnements
12 Benthiques (LECOB), 66650 Banyuls-sur-Mer, France

13 (b) Sorbonne Université, CNRS, FR3724, Observatoire Océanologique de Banyuls, 66650 Banyuls-
14 sur-Mer, France

15 (c) Réserve Naturelle Nationale de la Forêt de la Massane, Sorbonne Université, UPMC Univ Paris
16 06, Observatoire Océanologique de Banyuls, 66650 Banyuls-sur-Mer, France

17 * corresponding author, email: charles@obs-banyuls.fr

18 **Abstract**

19 Rivers transport a wide variety of materials, ranging from submillimeter-sized sediment particles
20 to entire trees. The transported deadwood constitutes a vital component of wooded river ecosystems.
21 The inputs of wood constantly alter the morphology of watercourses and influence river flow. Given the
22 inherently complex and diverse nature of river systems, a thorough exploration of their diversity is
23 justified to identify recurring trends in the dynamics of deadwood transport. This need becomes
24 imperative in regions already facing prolonged episodes of drought, frequent heatwaves, and an
25 increase in extreme precipitation events. In the specific context of the Massane River, a small
26 Mediterranean mountain river, our study aimed to lay the groundwork for a long-term monitoring of
27 deadwood transport by the watercourse. We began by conducting an inventory of large woody debris
28 present in the riverbed. Subsequently, we adapted an RFID-based tracking system to monitor deadwood
29 movement. Finally, we measured the distances traveled by wood pieces displaced following the initial
30 rise in water levels, a consequence of RFID tagging of wood pieces. This sequential approach indicated
31 that approximately one-third of the total deadwood stock volume was likely to be transported during
32 an ordinary flood event. The use of RFID technology effectively enabled the downstream tracking of
33 wood movement and revealed that even a moderate flood event could transport recently deposited
34 wood pieces nearly 4 kilometers. This work marks the initiation of a long-term monitoring effort to trace
35 the movement of deadwood from the river's source to its estuary and examine the relationship between
36 flood event types and the extent of wood transport.

37

38 **Keywords:** Rivers, Runoff, Floods, Large woody debris, Coarse wood, Radio telemetry, **Tracking,**
39 Displacement length

40

41 Version française

42 **Résumé**

43 Les rivières transportent une grande variété de matériaux, allant des particules de sédiments
44 de taille submillimétrique aux arbres entiers. Le bois mort transporté constitue un élément vital des
45 écosystèmes fluviaux boisés. Les apports de bois modifient constamment la morphologie des cours
46 d'eau et influent sur le débit fluvial. Étant donné la nature intrinsèquement complexe et diversifiée des
47 systèmes fluviaux, une exploration approfondie de leur diversité est justifiée pour identifier les
48 tendances récurrentes dans la dynamique du transport du bois mort. Ce besoin devient impératif dans
49 les régions déjà confrontées à des épisodes prolongés de sécheresse, des vagues de chaleur fréquentes

50 et une augmentation des événements de précipitations extrêmes. Dans le contexte spécifique de la
51 rivière de la Massane, une petite rivière de montagne méditerranéenne, notre étude visait à poser les
52 bases d'une surveillance à long terme du transport du bois mort par le cours d'eau. Nous avons
53 commencé par réaliser un inventaire des débris ligneux volumineux présents dans le lit de la rivière. Par
54 la suite, nous avons adapté un système de suivi basé sur la technologie RFID pour surveiller le
55 mouvement du bois mort. Enfin, nous avons mesuré les distances parcourues par les morceaux de bois
56 déplacés suite à la montée initiale du niveau de l'eau, conséquence du marquage RFID des morceaux de
57 bois. Cette approche séquentielle a indiqué qu'environ un tiers du volume total du stock de bois mort
58 était susceptible d'être transporté lors d'un événement de crue ordinaire. L'utilisation de la technologie
59 RFID a efficacement permis le suivi aval du mouvement du bois et a révélé qu'un événement de crue
60 modéré pouvait transporter des morceaux de bois récemment déposés sur près de 4 kilomètres. Ce
61 travail marque le début d'un effort de surveillance à long terme visant à retracer le mouvement du bois
62 mort depuis la source de la rivière jusqu'à son estuaire et à examiner la relation entre les types
63 d'événements de crue et l'étendue du transport du bois.

64 INTRODUCTION

65 The deadwood plays a key role in the functioning of habitats that succeed along the land-to-sea
66 continuum (Maser and Sedell, 1994; Naiman et al., 1999). Fallen branches and trees in riparian forests
67 create structurally rich riverbanks (Naiman and Décamps, 1997), offering habitats for various species
68 including insects (Parisi et al., 2021), amphibians (Herbeck and Larsen, 1999), mammals (Radu, 2006),
69 and birds (Mikusinski and Angelstam, 1997). Deadwood's role persists as it enters the riverbed,
70 providing crucial shelter, spawning areas, and foraging opportunities for aquatic life (Angermeier and
71 Karr, 1984; Anderson et al., 1984). Releasing organic substances, deadwood also contributes to major
72 biogeochemical cycles, enriching surrounding water with essential nutrients (Bilby and Likens, 1980).
73 Downstream, deadwood maintains its ecological importance (Sleeter and Coull, 1973) and served as a
74 long-term carbon sink (Canuel and Hardison, 2016), contributing to climate change mitigation (McLeod
75 et al., 2011; Russell et al., 2015; Zeng, 2008).

76 Rivers act as natural conduits for large woody debris (Harmon et al., 1986). A comprehensive
77 understanding of the dynamics of deadwood transport in rivers is crucial for identifying areas prone to
78 debris accumulation (Comiti et al., 2016). This knowledge provides the necessary foundation for
79 developing strategies for flood mitigation and responding to extreme flood events (Mazzorana et al.,
80 2018; Nicholson et al., 2012).

81 Any efforts to characterize the spatial distribution and transport of deadwood in river systems
82 provide valuable insights into the natural processes that shape river environments (Pedroli et al., 2002).
83 These insights, in turn, guide initiatives related to river restoration and biodiversity conservation (Roni
84 et al., 2015; Wohl et al., 2015). Quantifying the temporal dynamics of wood in rivers can be achieved
85 using various techniques (MacVicar et al., 2009). Among these, individual tracking techniques offer
86 valuable assessments of wood mobilization, deposition, and transport distance. Visual methods, such
87 as the recognition of individual pieces based on shape, location, and the presence of distinctive features
88 of the debris (Lienkaemper and Swanson, 1987), as well as labeling wood pieces with waterproof acrylic
89 paints (Jacobson et al., 1999) or using vinyl plastic number tags for identification (Haga et al., 2002),
90 have provided valuable information on individual wood movement. However, these visual methods are
91 limited in accuracy and durability. In contrast, radio telemetry using RFID facilitates real-time data
92 collection through remote sensing, enables precise location tracking of multiple pieces of deadwood
93 simultaneously (Schenk et al., 2014), all without frequent replacements or maintenance efforts.

94 Originally conceived to enhance military radar systems (Hanbury Brown, 1994), RFID has
95 evolved into a widely utilized practical identification tool across various fields, including logistics, supply
96 chain management, and ecological conservation. RFID technology has played an important role in

97 monitoring animal movements, migration patterns, and behaviors, providing valuable insights for
98 habitat preservation and species conservation (Harrison and Kelly, 2022; Kissling et al., 2014; Skov et al.,
99 2008). More recently, their use in tracking the movement of wood (MacVicar et al., 2009; Ravazzolo et
100 al., 2015; Schenk et al., 2014) and pebbles (Cassel et al., 2020, 2017) has expanded their range of
101 applications to the study of processes in river environments.

102 In the present work, we relied on this approach for characterizing the transport of deadwood
103 along a small mountainous forested Mediterranean river. The Mediterranean forests, despite covering
104 only a small area of the world's forests, harbor a remarkable diversity of woody species (Gauquelin et
105 al., 2018). However, climate change poses challenges as this region experiences shifts in precipitation
106 patterns, with overall decreases in precipitation and an increase in extreme rainfall (Zittis et al., 2019).
107 River flow and discharge are expected to decrease significantly, leading to water scarcity, more frequent
108 droughts and severe flood events (Tramblay and Somot, 2018). These changes are likely to influence
109 the timing and magnitude of wood inputs, causing fluctuations in wood transport and deposition
110 dynamics within these river systems.

111 The overall objective of this study is to initiate RFID tracking to monitor the mobility of
112 deadwood in the Massane River, a small mountainous river that originates in the foothills of the French
113 Pyrenees and flows into the Mediterranean Sea. The study aims to achieve three specific objectives:
114 quantifying the distribution of deadwood in the riverbed, developing an RFID tracking protocol for
115 individual pieces of deadwood in a forested and rugged environment, and gaining insights from the first
116 significant flood event that resulted in the movement of the RFID-tagged deadwood pieces.

117

118 MATERIAL AND METHODS

119 Study site

120 The Massane River, depicted in Figure 1, originates at an elevation of 970 meters in the Eastern
121 Pyrenees foothills and meanders for 22.02 kilometers before it reaches the Mediterranean Sea. The
122 watershed area covering this region spans 17.2 square kilometers. As the river flows from its source to
123 the confluence with the Source of Alemanys at an elevation of 610 meters, it traverses the National
124 Nature Reserve of the Massane Forest (336 ha), covering a distance of 5.2 kilometers. In this particular
125 section, the river exhibits a steep gradient of 6.5%, flanked by 18.4 hectares of riparian forest. The most
126 prevalent tree species in this area are beech (*Fagus sylvatica*) and alder (*Alnus glutinosa*). While beech
127 trees can be found throughout this section of the river, alder trees are limited to altitudes below 800
128 meters.

129

130 **Deadwood stock in the upper river stretch**

131 In June 2021, a survey was conducted in the river section that crosses through the reserve, as
132 shown in Figure 1. The purpose of the survey was to assess the quantity and distribution of deadwood
133 along the watercourse. The surface area of the channel in this section of the river is estimated to be 4.9
134 hectares. Data collection involved measuring various parameters for each piece of wood found in the
135 riverbed, including length, average diameter, tree species, degradation state, and geographical position.
136 The measurements of individual wood pieces, including fallen tree trunks and branch sections, were
137 used to calculate volumes using a cylinder equation. Deadwood was quantified as cubic meters per
138 hectare ($\text{m}^3 \text{ha}^{-1}$) and pieces per hectare (pieces ha^{-1}).

139 For this study, deadwood was defined as individual logs with dimensions of at least 0.1 meters in
140 diameter and 0.4 meters in length. This specific definition was chosen to standardize wood size in
141 relation to the stream bank's full width (Comiti et al., 2006). In certain areas, like Lavail Gorge, the river
142 narrows significantly, with a distance of only 2.5 meters between the rocky walls that enclose the
143 waterway. To assess the degradation process, a scale from 1 to 4 was used to characterize the decay
144 stage of the deadwood pieces. The state of decay was determined based on external appearance and
145 wood density, as follows:

- 146 • Stage 1: Recently recruited pieces of dense wood with intact bark, leaves, or buds at the ends
147 of branches.
- 148 • Stage 2: Dense wood with more than 70% of its bark intact and no signs of abrasion from river
149 scouring.
- 150 • Stage 3: Pieces of wood that are still dense, have spent several months in the riverbed, lost
151 more than 70% of their bark, and show clear signs of abrasion.
- 152 • Stage 4: Completely rotten wood that decomposes upon contact or under weak pressure.

153 Stages 1, 2, and 3 represent deadwood that can be mobilized during floods, while Stage 4 represents
154 non-transportable wood that will inevitably decay when the river rises again. Stages 1 and 2 specifically
155 capture recent recruitment of deadwood into the river.

156

157 **RFID tracking in the field**

158 *RFID system description*

159 RFID technology, originally developed for managing inventory, logistics, and various applications
160 like microchipping domestic animals, gates, and access points, is typically employed in scenarios where
161 the tagged object is mobile, while the reader, connected to a powered main PC, remains stationary.
162 Although embedded solutions exist, they often require carrying a laptop or tablet, which can be
163 cumbersome, power-consuming, and fragile. Due to the absence of an off-the-shelf solution, we
164 undertook the development of a lightweight and compact reading device designed for pedestrian use
165 over long distances in rugged natural environments (Plate I).

166 In our system, we utilized active RFID tags equipped with onboard batteries, enabling signal
167 exchanges at a frequency of 433.92 MHz over distances of up to 100 meters. To capture, read, and
168 record the information received by the receiver, we employed an Arduino AT Mega 2560
169 microcontroller board. The RS232 PC serial port signals from the RFID reader were converted into logic-
170 level data using a serial adapter RS232/TTL module connected to the universal asynchronous reception
171 and transmission (UART) serial port 1 of the board. Subsequently, the identification number and
172 received signal strength indicator (RSSI) level of the detected tag were displayed in real-time via the I2C
173 (Integrated Circuit Interface) port of the microcontroller on an LCD I2C 20x40 Arduino module (Plate I).
174 Data was further stored on a micro SD card as a text file using a micro-SD reader/writer module
175 connected to the serial peripheral interface (SPI) port of the microcontroller. The recording frequency
176 matched the emission rate of the tags, which transmitted one signal every 2 seconds. Each acquisition
177 was timestamped and included latitude and longitude data collected from a GPS module (Adafruit
178 Ultimate GPS Breakout) connected to the UART2 port of the AT Mega board. A 12V 6800 mA
179 rechargeable li-ion battery provided power for the system, enabling operation for more than 8 hours.
180 The complete detection system, including the protective casing, had a weight of 550 grams and
181 dimensions of 13x12x12 cm.

182 All RFID equipment used in this study was designed by ELA Innovation in France. The tags
183 employed were PUCK IDs® tags, the receiver was the SCIEL READER lite® reader, and the antenna used
184 was the semi-directional SLENDER III® antenna. Detailed technical specifications can be found on the
185 manufacturer's website at <https://elainnovation.com/>. We procured the equipment from the CIPAM
186 company.

187

188 *Experimental Setup*

189 The tagged wood used in the experiment consisted of beech logs measuring 0.6 m in length and
190 ranging in diameter from 0.11 to 0.15 m. A total of fifty freshly cut logs were equipped with RFID tags,
191 each with a base measuring 57 mm and a height of 20 mm (Plate I). These RFID tags were inserted into

192 pre-drilled slots in the wood and securely affixed using silicone glue. On July 17, 2021, starting from the
 193 source of the river, these tagged wood logs were systematically placed at 100-meter intervals along the
 194 riverbed.

195 After installation and prior to the occurrence of the next flood event, data collection involved
 196 measuring the received signal strength indicator (RSSI) levels at various distances within the study
 197 environment. This data collection aimed to capture the signal propagation patterns within the complex
 198 terrain of the study site while ensuring the RFID tags remained operational. The data files recorded by
 199 the reading systems were processed to calculate the distances between different detector positions and
 200 the tagged wood logs. These distances were determined using the Haversine equation, which accounts
 201 for the curvature of the Earth.

202 To characterize the attenuation of RSSI as the radio signal propagates, we employed a simplified
 203 equation based on the Free Space Path Loss (FSPL) model, as shown below:

$$204 \quad \text{RSSI} = \text{RSSI}_0 - 10 \times n \times \log_{10}(d) \quad (1)$$

205 *RSSI* represents the received signal strength indicator level. *RSSI₀* is the received signal strength level
 206 at a reference distance of 1 meter. *n* is the attenuation parameter, which is a parameter that determines
 207 the rate of power decrease of the signal with distance. *d* is the distance, in meters, between the
 208 transmitter and receiver of the signal. The parameter *n* can vary depending on the environment,
 209 obstacles, and propagation path characteristics. In a free space environment, without obstacles or
 210 reflections, the typical value of *n* is generally close to 2.

211

212 **Analysis of tag travel distances and transport outcomes**

213 After the initial significant rainfall events that occurred following the installation of the tags, we
 214 conducted surveys along the river to locate the marked wood logs. Using the data collected by the RFID
 215 reading system, we retrieved the GPS coordinates corresponding to the reader's position that
 216 corresponded to the best-recorded RSSI level for each tag.

217 To determine the distances covered by the tags, we obtained the geo-referenced course of the
 218 river from the repository maintained by the French national administration service for water data
 219 (<http://www.sandre.eaufrance.fr/geo/CoursEau/Y0110540>). We then applied the Haversine formula to
 220 calculate the distances between consecutive points on this route. By summing the lengths of these
 221 consecutive intervals, we could calculate the distance between each geo-referenced point on the river
 222 and the position of the river's source.

223 With knowledge of the distance between the source and the tag at time 't' (i.e., before the
224 rainfall event) and the distance at time 't+dt' (i.e., after the rainfall event), we were able to calculate the
225 travel distance of the tags during the time interval 'dt' by taking the difference between the two
226 distances. The assessment of wood transport was quantified in terms of meters traveled per flood event.
227 Additionally, we carefully recorded whether the logs ended up isolated or in a logjam, either within or
228 outside the river's main channel after their transport.

229

230 RESULTS

231 Deadwood distribution and quantification

232 The survey conducted in June 2021 revealed that a total of 368 pieces of wood, equivalent to
233 75 pieces per hectare (ha^{-1}), were present in the channel of the upper river stretch, representing a
234 combined volume of 32.9 m^3 ($7.7 \text{ m}^3 \text{ ha}^{-1}$) (Figure 2). Across the entire 5.2-kilometer stretch of the river,
235 these wood pieces were distributed widely. Only a few areas, notably near the Couloumates cabins
236 (Figure 2A), were observed to have a scarcity of deadwood.

237 The majority of the deadwood, both in terms of the number of pieces and volume, originated
238 from beech trees (82-78%) and alder trees (12-13%). Wood pieces with a length smaller than the width
239 of the river at its narrowest point, which is 2.5 meters, constituted 74% of the counts and 34% of the
240 total deadwood volume (Figure 2B). The most common state of degradation observed was stage 3,
241 characterized by wood pieces that had spent some time in the riverbed, shedding over 70% of their
242 bark, and displaying evident signs of abrasion. This stage accounted for 85% of the overall deadwood
243 volume. Stage 4, indicative of completely rotten wood, comprised 6% of the total deadwood volume.

244

245 RFID tracking

246 Between the completion of the inventory and September, there were no rainfall events that
247 caused the marked logs to move. During this period, the recordings of RFID tag signals in the intricate
248 study site environments showed notable background noise. This led to very low received signal strength
249 indicator (RSSI) measurements for short distances between RFID tags and the reader, as illustrated in
250 Figure 3A. This was partly due to the presence of obstacles that weakened the signal's range but
251 primarily because the reader's reception antenna was semi-directional. Consequently, when the
252 antenna was not aligned with the tag, the RSSI value decreased. To address this issue and apply the
253 signal attenuation model, we filtered the data to retain only the highest RSSI values within a 5-meter
254 range (Figure 3A).

255 This analysis, conducted on all the tags in place at the time of measurement (Figure 3B),
256 indicated that the best RSSI value was around -90 dB. The average value of the attenuation parameter,
257 'n,' was 5.1, with extreme values ranging from 3.5 to 6.7, and a mean detection range of 134 meters,
258 lying between the extreme values of 73 and 220 meters.

259 The monitoring of the tags allowed us to detect that one tag went missing in the vicinity of the
260 Couloumates cabins, and two others malfunctioned before the onset of the first flood. We replaced the
261 faulty tags, while the missing one was not replaced.

262

263 **Tag travel distances**

264 Initially, starting from the source, tagged wood logs were positioned at 100-meter intervals in
265 the riverbed (Figure 4A). An episode of rainfall occurred on September 16th and 18th, 2021. The daily
266 precipitation accumulations recorded at the meteorological station within the reserve during these days
267 did not exceed 22 mm per day. However, the cumulative effect was substantial enough to induce the
268 movement of deadwood within the river. The position of the tags after this event (Figure 4B) indicates
269 that the majority of the marked logs were displaced, sometimes over long distances. Three marked
270 wood pieces exited the reserve boundaries.

271 The observed maximum value was 3840 meters (Figure 5). Individual analysis of travel distances
272 confirmed that nearly all of the marked pieces moved, some (e.g., tags 2B3, 2BD, 2DB, 2E2) by a few
273 meters, and others (e.g., tags 2B9, 2C3, 2D3, 2E1) over several kilometers. The median value was 790
274 meters. Fifty percent of the tagged wood travelled between 330 m and 1550 m. Deadwood that was
275 susceptible to transport was mobilized by the rising water level, with no observable effect of the initial
276 position of the wood piece on the distance traveled. Of the logs, half ended up isolated, while the other
277 half became part of logjams. Location categorization revealed that 65% remained within the river's main
278 channel, while 35% were deposited outside the main channel after transport.

279

280 **DISCUSSION**

281 **Reflections on study scope**

282 Our study provides quantitative insights into the stock and condition of deadwood in a small
283 coastal Mediterranean mountainous river. It demonstrates the efficiency of RFID tracking in **evaluating**
284 deadwood mobility and introduces additional findings on the transport of these materials following an
285 initial flood event. However, it is essential to consider these results within the context of inherent
286 limitations stemming from methodological choices. These limitations encompass the dimensions and
287 context of deadwood assessment in the riverbed, the reliability of the RFID tracking equipment, and the

288 sampling and methodology used to evaluate deadwood transport. Firstly, the selected dimensions of
289 deadwood logs may influence the interpretation of the total deadwood stock in the river. However, this
290 choice does not undermine the main findings of our study, which primarily focused on 'large wood
291 debris' significantly impacting fluvial dynamics. Besides, this decision enables a comparative analysis
292 with data previously collected by the reserve's managers (Magdalou et al., 2009). A minor yet tangible
293 limitation concerns the reliability of the RFID tracking equipment. Malfunctions, such as the lack of
294 waterproofness of tags or unexpected battery depletion, may affect result precision and data
295 interpretation. The interpretation of signal loss in cases where a wood piece was not retrieved raised
296 questions about the possibility of it being transported beyond search limits or ceasing activity without
297 movement. Without visual confirmation of the presence of a wood piece that was no longer emitting a
298 radio signal, we assumed that the last flood event had caused its movement. However, the tagged log
299 was excluded from further tracking. Nevertheless, such incidents fortunately remained infrequent. The
300 final limitation pertains to the sampling and methodology employed to evaluate deadwood transport.
301 This includes the introduction of specific logs, which might not precisely emulate the behavior of
302 naturally occurring deadwood. While this limitation narrows our focus to recently recruited isolated
303 deadwood stocks, rather than encompassing the entire stock in the river, our findings hold value in
304 addressing this specific aspect. The approach also holds significance as it initiates a tracking process for
305 deadwood from its entry into the riverbed, adding another dimension to our understanding of its
306 mobility.

307

308 **Main study findings**

309 *Deadwood stocks*

310 Our study revealed a significant decline in both the number of deadwood pieces and the total
311 volume of deadwood in the river when compared to data recorded between 2001 and 2008 (Magdalou
312 et al., 2009). Additionally, the observed ongoing trend of increased predominance of beech and alder
313 at the expense of other tree species at that time has become more pronounced. These differences and
314 shifts reflect natural variability in annual wood inputs and river flows emphasizing the amplified impact
315 of climatic disturbances on tree mortality and the decline in the riparian forest stand.(Allen et al., 2010;
316 Carnicer et al., 2011; Ruiz-Benito et al., 2013).

317 The river's narrow width acts as a natural filter, allowing primarily wood pieces smaller than 2.5
318 meters in length to be transported over long distances during annual floods. Nevertheless, the amount
319 of deadwood mobilized by an annual flood remains substantial, representing approximately one-third
320 of the total stock volume, according to our estimates. The tagged wood pieces used in our study

321 provided valuable insights into the maximum distances that logs can travel during floods, as small
322 isolated logs are more responsive to changes in water flow and may travel longer distances compared
323 to larger logs (Ruiz-Villanueva et al., 2016).

324

325 *RFID Reliability*

326 During the current survey, the recovery rate of tagged logs reached 96%, a figure higher than
327 typically reported in the literature (MacVicar et al., 2009; Ravazzolo et al., 2015; Schenk et al., 2014).
328 This performance can be attributed to two key factors: pre-flood monitoring of the RFID beacon group
329 and the river's configuration. The monitoring of RFID beacons before the flood event ensured the
330 continued activity of the maximum number of tagged logs. Furthermore, the Massane River, being a
331 small river with a single channel, significantly simplified the process of recovering tagged wood pieces
332 by reducing the width of possible search areas. The RFID tag reading system demonstrated remarkable
333 robustness in traversing the river. The RFID signal interpretation and recording module, weighing less
334 than 600 g, accounted for only a small fraction of the total weight of the reading system, which included
335 the 2 kg detection antenna. However, this weight discrepancy was compensated by the antenna's
336 excellent long-distance detection capabilities. Despite variations in the maximum detection range from
337 one RFID tag to another due to natural obstacles and wave reflections disrupting the radio signal
338 propagation locally, the system consistently performed well. The 'n' values for the attenuation
339 parameter were consistently higher than the characteristic value for signal propagation in an obstacle-
340 free open space. Values exceeding 5 should be considered relative, as they are rarely achievable in real-
341 world conditions. These artifacts result from the limitations of the model used to represent the datasets
342 collected for certain tags. Typically, the recovered logs were visually confirmed. In all instances, a higher
343 or near -120 dB RSSI value indicated the presence of the marked log within a distance of less than 10
344 meters. With GPS measurements having an accuracy of about 5 meters, the badge's position could be
345 determined with a margin of error of less than 15 meters in the worst-case scenario.

346 *Wood mobility*

347 We observed a significant absence of deadwood in the river section adjacent to the
348 Couloumates cabins (Figure 2A). Notably, one of our tagged logs disappeared before any rise in the
349 river's water level. This particular area serves as a bivouac site for hikers. Despite our efforts to locate
350 the log for which we had the GPS position, we suspect that the log, along with its RFID tag, might have
351 been removed from the river to be burned. However, apart from this unexpected incident, the RFID
352 monitoring proved to be effective and precise.

353 The rise in river water levels following the September rainfall prompted the displacement of
354 almost all marked pieces. In contrast to previous studies based on introduced wood in steep-gradient
355 watercourses (Millington and Sear, 2007, and others), our research reveals the potential for wood to
356 travel considerable distances—up to 17% of the river's total length—even with a minor increase in the
357 water level (Steeb et al., 2017). The arrangement of the logs, initially evenly spaced along the
358 watercourse into the riverbed, was significantly altered, revealing areas with varying degrees of
359 clustering. Wood logs were transported downstream until they were deposited either on rock outcrops,
360 incorporated into logjams, or ejected onto the banks outside the riverbed. These positions assumed a
361 more natural state (Plate II), indicating a stability gradient likely developed due to the transport and
362 deposition conditions of the wood pieces. This new situation provides a more accurate representation
363 of flood-induced changes in deadwood mobility.

364 Following this initial movement, 37% of the pieces remain isolated in the riverbed, highly
365 mobilizable, and 28% caught in a logjam inside the main channel of the river can be considered as
366 potentially easily mobilizable during a typical flood event. Pieces of wood trapped in logjams or
367 deposited on the riverbanks can be remobilized during more intense flood events, provided these flood
368 events occur before the degradation process is complete. This is highly probable since it takes at least a
369 decade for a piece of beech wood to completely degrade in this environment (Charles et al., 2022).
370 Continuing the monitoring will help determine the pace at which deadwood continues its downstream
371 journey and whether flood intensity and contextual factors (isolated/trapped-in-a-logjam; in/out of the
372 riverbed) influence the mobilization and transport of wood (Oettel et al., 2022).

373 The daily precipitation accumulations that triggered the movement of deadwood were relatively low.
374 The measuring station located at Mas d'en Tourens, 14 km from the source, did not record any
375 significant rise in the water level. These precipitation events followed a long period of drought, resulting
376 in substantial runoff. The rains were brief but intense enough to cause a noticeable rise in the water
377 level in the upper reaches of the watercourse. This event, by causing the disintegration of water
378 reservoirs formed by logjams and the creation of new ones, had a localized effect on both accelerating
379 and slowing down the river's flow rate. These observations highlight the challenge of linking deadwood
380 movement to flood events, emphasizing the localized effects of precipitation even in small-scale areas.

381

382 **Implications of the study**

383 Understanding the storage of deadwood, the processes governing it, and the dynamics of its
384 transport is a prerequisite for the choice of effective river management strategies, particularly in the
385 face of significant climate changes (Benda and Sias, 2003). Such strategies aim to reduce the risk of

386 watercourse obstruction, enhance flood prevention measures, and support river restoration efforts
387 (Wohl et al., 2015). In the context of our study, which focuses on a small coastal Mediterranean
388 mountainous river in its natural state, several key observations are worth highlighting. A substantial
389 portion of the deadwood in this river consists of relatively small pieces. When isolated within the
390 riverbed, these pieces have the potential for long-distance transportation even during minor water level
391 rising events. The river's narrow width leads to the fragmentation of larger tree pieces before they can
392 be transported. This fragmentation process reduces the risks typically associated with exceptionally
393 large pieces that could damage infrastructure. Occurrences of logjams and resulting barriers in the river
394 play a crucial role in mitigating the impacts of rising water levels during flood events. These logjams
395 contribute to the natural regulation of river flow and help preserve essential stream habitats. This work
396 sets the stage for the continuation of investigations, determining whether the tagged wood pieces will
397 persist in their downstream journey. It aims to establish a clear link between the intensity of flood events
398 and induced movements, while also evaluating the durability of RFID tagging. In essence, these initial
399 findings underscore the importance of preserving natural river environments with minimal human
400 intervention. Allowing natural processes, such as deadwood accumulation and logjam formation, to
401 continue enhances the resilience of river ecosystems and their ability to manage flood events
402 effectively. This approach aligns with sustainable river management practices and contributes to the
403 overall health and stability of these vital ecosystems.

404

405 **Acknowledgments**

406 This research, part of the Xyloscope project coordinated by FC, has been made possible through
407 the support of the French national program EC2CO (Continental and Coastal Ecosystem). We would like
408 to extend our sincere gratitude to several individuals for their invaluable contributions to this research.
409 First and foremost, we express our appreciation to Mr. Bernard Latour from the Office National des
410 Forêts for generously providing the wooden pieces crucial to this study. Special thanks are extended to
411 Esther for her dedicated efforts in installing the pieces in the river, Philippe for his valuable assistance
412 during field research, and Hippolyte for his significant contributions to data extraction and formatting.
413 Additionally, we would like to acknowledge the opportunity to present the findings of this manuscript
414 at the colloquium celebrating the 50th anniversary of the Forêt de la Massane, held from November 22
415 to 24, 2023, at the Observatoire Océanologique de Banyuls. This event, expertly organized by Elodie
416 Magnanou and Diane Sorel, provided a platform to share and discuss the research. We express our
417 heartfelt gratitude to Elodie and Diane for their kind invitation and the opportunity to be part of this
418 memorable event.

419

420

421 **Literature cited**

- 422 Allen, C.D., Macalady, A.K., Chenchouni, H., Bachelet, D., McDowell, N., Vennetier, M., Kitzberger, T.,
423 Rigling, A., Breshears, D.D., Hogg, E.H. (Ted), Gonzalez, P., Fensham, R., Zhang, Z., Castro, J., Demidova,
424 N., Lim, J.-H., Allard, G., Running, S.W., Semerci, A., Cobb, N., 2010. A global overview of drought and
425 heat-induced tree mortality reveals emerging climate change risks for forests. *For. Ecol. Manag.* 259,
426 660–684. <https://doi.org/10.1016/j.foreco.2009.09.001>
- 427 Anderson, N.H., Steedman, R.J., Dudley, T., 1984. Patterns of exploitation by stream invertebrates of
428 wood debris (xylophagy): With 2 figures and 2 tables in the text. *SIL Proc.* 1922-2010 22, 1847–1852.
429 <https://doi.org/10.1080/03680770.1983.11897584>
- 430 Benda, L.E., Sias, J.C., 2003. A quantitative framework for evaluating the mass balance of in-stream
431 organic debris. *For. Ecol. Manag.* 172, 1–16. [https://doi.org/10.1016/S0378-1127\(01\)00576-X](https://doi.org/10.1016/S0378-1127(01)00576-X)
- 432 Bilby, R.E., Likens, G.E., 1980. Importance of Organic Debris Dams in the Structure and Function of
433 Stream Ecosystems. *Ecology* 61, 1107–1113. <https://doi.org/10.2307/1936830>
- 434 Canuel, E.A., Hardison, A.K., 2016. Sources, Ages, and Alteration of Organic Matter in Estuaries. *Annu.*
435 *Rev. Mar. Sci.* 8, 409–434. <https://doi.org/10.1146/annurev-marine-122414-034058>
- 436 Carnicer, J., Coll, M., Ninyerola, M., Pons, X., Sánchez, G., Peñuelas, J., 2011. Widespread crown
437 condition decline, food web disruption, and amplified tree mortality with increased climate change-
438 type drought. *Proc. Natl. Acad. Sci.* 108, 1474–1478. <https://doi.org/10.1073/pnas.1010070108>
- 439 Cassel, M., Dépret, T., Piégay, H., 2017. Assessment of a new solution for tracking pebbles in rivers
440 based on active RFID: A NEW SOLUTION FOR TRACKING PEBBLES IN RIVERS BASED ON ACTIVE RFID.
441 *Earth Surf. Process. Landf.* 42, 1938–1951. <https://doi.org/10.1002/esp.4152>
- 442 Cassel, M., Piégay, H., Fantino, G., Lejot, J., Bultingaire, L., Michel, K., Perret, F., 2020. Comparison of
443 ground-based and UAV a-UHF artificial tracer mobility monitoring methods on a braided river. *Earth*
444 *Surf. Process. Landf.* 45, 1123–1140. <https://doi.org/10.1002/esp.4777>
- 445 Comiti, F., Lucía, A., Rickenmann, D., 2016. Large wood recruitment and transport during large floods:
446 A review. *Geomorphology* 269, 23–39. <https://doi.org/10.1016/j.geomorph.2016.06.016>
- 447 Gauquelin, T., Michon, G., Joffre, R., Duponnois, R., Génin, D., Fady, B., Bou Dagher-Kharrat, M.,
448 Derridj, A., Slimani, S., Badri, W., Alifriqui, M., Auclair, L., Simenel, R., Aderghal, M., Baudoin, E.,
449 Galiana, A., Prin, Y., Sanguin, H., Fernandez, C., Baldy, V., 2018. Mediterranean forests, land use and
450 climate change: a social-ecological perspective. *Reg. Environ. Change* 18, 623–636.
451 <https://doi.org/10.1007/s10113-016-0994-3>
- 452 Haga, H., Kumagai, T., Otsuki, K., Ogawa, S., 2002. Transport and retention of coarse woody debris in
453 mountain streams: An in situ field experiment of log transport and a field survey of coarse woody
454 debris distribution: COARSE WOODY DEBRIS IN MOUNTAIN STREAMS. *Water Resour. Res.* 38, 1-1-1–
455 16. <https://doi.org/10.1029/2001WR001123>
- 456 Hanbury Brown, R., 1994. Robert Watson-Watt, the Father of Radar. *Eng. Sci. Educ. J.* 3, 31–40.
- 457 Harmon, M.E., Franklin, J.F., Swanson, F.J., Sollins, P., Gregory, S.V., Lattin, J.D., Anderson, N.H., Cline,
458 S.P., Aumen, N.G., Sedell, J.R., Lienkaemper, G.W., Cromack, K., Cummins, K.W., 1986. Ecology of
459 coarse woody debris in temperate ecosystems, in: *Advances in Ecological Research*. Elsevier, pp. 59–
460 234. [https://doi.org/10.1016/S0065-2504\(03\)34002-4](https://doi.org/10.1016/S0065-2504(03)34002-4)

- 461 Harrison, N.D., Kelly, E.L., 2022. Affordable RFID loggers for monitoring animal movement, activity, and
462 behaviour. *PLOS ONE* 17, e0276388. <https://doi.org/10.1371/journal.pone.0276388>
- 463 Herbeck, L.A., Larsen, D.R., 1999. Plethodontid Salamander Response to Silvicultural Practices in
464 Missouri Ozark Forests. *Conserv. Biol.* 13, 623–632. [https://doi.org/10.1046/j.1523-
465 1739.1999.98097.x](https://doi.org/10.1046/j.1523-1739.1999.98097.x)
- 466 Jacobson, P.J., Jacobson, K.M., Angermeier, P.L., Cherry, D.S., 1999. Transport, Retention, and
467 Ecological Significance of Woody Debris within a Large Ephemeral River. *J. North Am. Benthol. Soc.* 18,
468 429–444. <https://doi.org/10.2307/1468376>
- 469 Kissling, W.D., Pattemore, D.E., Hagen, M., 2014. Challenges and prospects in the telemetry of insects:
470 Insect telemetry. *Biol. Rev.* 89, 511–530. <https://doi.org/10.1111/brv.12065>
- 471 Lienkaemper, G.W., Swanson, F.J., 1987. Dynamics of large woody debris in streams in old-growth
472 Douglas-fir forests. *Can. J. For. Res.* 17, 150–156. <https://doi.org/10.1139/x87-027>
- 473 MacVicar, B.J., Piñay, H., Henderson, A., Comiti, F., Oberlin, C., Pecorari, E., 2009. Quantifying the
474 temporal dynamics of wood in large rivers: field trials of wood surveying, dating, tracking, and
475 monitoring techniques. *Earth Surf. Process. Landf.* 34, 2031–2046. <https://doi.org/10.1002/esp.1888>
- 476 Magdalou, J.-A., Hurson, C., Garrigue, J., 2009. Dynamique du bois mort et impact des crues sur
477 quelques espèces riveraines. *Trav. Réserve Nat. Massane Travaux de la Massane n°80*, 33.
- 478 Maser, C., Sedell, J.R., 1994. From the forest to the sea: the ecology of wood in streams, rivers,
479 estuaries, and oceans. St. Lucie Press, Delray Beach, FL.
- 480 Mazzorana, B., Ruiz-Villanueva, V., Marchi, L., Cavalli, M., Gems, B., Gschnitzer, T., Mao, L., Iroumé, A.,
481 Valdebenito, G., 2018. Assessing and mitigating large wood-related hazards in mountain streams:
482 recent approaches. *J. Flood Risk Manag.* 11, 207–222. <https://doi.org/10.1111/jfr3.12316>
- 483 Mcleod, E., Chmura, G.L., Bouillon, S., Salm, R., Björk, M., Duarte, C.M., Lovelock, C.E., Schlesinger,
484 W.H., Silliman, B.R., 2011. A blueprint for blue carbon: toward an improved understanding of the role
485 of vegetated coastal habitats in sequestering CO₂. *Front. Ecol. Environ.* 9, 552–560.
486 <https://doi.org/10.1890/110004>
- 487 Mikusinski, G., Angelstam, P., 1997. European woodpeckers and anthropogenic habitat change: a
488 review. *Vogelwelt* 277–283.
- 489 Naiman, R.J., Balian, E.V., Bartz, K.K., Latterell, J.J., 1999. Dead Wood Dynamics in Stream Ecosystems,
490 in: *Proceedings of the Symposium on the Ecology and Management of Dead Wood in Western Forests*.
491 pp. 23–48.
- 492 Naiman, R.J., Décamps, H., 1997. The Ecology of Interfaces: Riparian Zones. *Annu. Rev. Ecol. Syst.* 28,
493 621–658. <https://doi.org/10.1146/annurev.ecolsys.28.1.621>
- 494 Nicholson, A.R., Wilkinson, M.E., O'Donnell, G.M., Quinn, P.F., 2012. Runoff attenuation features: a
495 sustainable flood mitigation strategy in the Belford catchment, UK. *Area* 44, 463–469.
496 <https://doi.org/10.1111/j.1475-4762.2012.01099.x>
- 497 Parisi, F., Innangi, M., Tognetti, R., Lombardi, F., Chirici, G., Marchetti, M., 2021. Forest stand structure
498 and coarse woody debris determine the biodiversity of beetle communities in Mediterranean
499 mountain beech forests. *Glob. Ecol. Conserv.* 28, e01637.
500 <https://doi.org/10.1016/j.gecco.2021.e01637>

- 501 Pedroli, B., de Blust, G., van Looy, K., van Rooij, S., 2002. Setting targets in strategies for river
502 restoration. *Landsc. Ecol.* 5–18.
- 503 Radu, S., 2006. The Ecological Role of Deadwood in Natural Forests, in: Gafta, D., Akeroyd, J. (Eds.),
504 Nature Conservation, Environmental Science and Engineering. Springer Berlin Heidelberg, Berlin,
505 Heidelberg, pp. 137–141. https://doi.org/10.1007/978-3-540-47229-2_16
- 506 Ravazzolo, D., Mao, L., Picco, L., Lenzi, M.A., 2015. Tracking log displacement during floods in the
507 Tagliamento River using RFID and GPS tracker devices. *Geomorphology* 228, 226–233.
508 <https://doi.org/10.1016/j.geomorph.2014.09.012>
- 509 Roni, P., Beechie, T., Pess, G., Hanson, K., 2015. Wood placement in river restoration: fact, fiction, and
510 future direction. *Can. J. Fish. Aquat. Sci.* 72, 466–478. <https://doi.org/10.1139/cjfas-2014-0344>
- 511 Ruiz-Benito, P., Lines, E.R., Gómez-Aparicio, L., Zavala, M.A., Coomes, D.A., 2013. Patterns and Drivers
512 of Tree Mortality in Iberian Forests: Climatic Effects Are Modified by Competition. *PLoS ONE* 8,
513 e56843. <https://doi.org/10.1371/journal.pone.0056843>
- 514 Ruiz-Villanueva, V., Piégay, H., Gurnell, A.M., Marston, R.A., Stoffel, M., 2016a. Recent advances
515 quantifying the large wood dynamics in river basins: New methods and remaining challenges: Large
516 Wood Dynamics. *Rev. Geophys.* 54, 611–652. <https://doi.org/10.1002/2015RG000514>
- 517 Ruiz-Villanueva, V., Wyżga, B., Zawiejska, J., Hajdukiewicz, M., Stoffel, M., 2016b. Factors controlling
518 large-wood transport in a mountain river. *Geomorphology* 272, 21–31.
519 <https://doi.org/10.1016/j.geomorph.2015.04.004>
- 520 Russell, M.B., Fraver, S., Aakala, T., Gove, J.H., Woodall, C.W., D'Amato, A.W., Ducey, M.J., 2015.
521 Quantifying carbon stores and decomposition in dead wood: A review. *For. Ecol. Manag.* 350, 107–
522 128. <https://doi.org/10.1016/j.foreco.2015.04.033>
- 523 Schenk, E.R., Moulin, B., Hupp, C.R., Richter, J.M., 2014. Large wood budget and transport dynamics
524 on a large river using radio telemetry. *Earth Surf. Process. Landf.* 39, 487–498.
525 <https://doi.org/10.1002/esp.3463>
- 526 Skov, C., Brodersen, J., Nilsson, P.A., Hansson, L.-A., Brönmark, C., 2008. Inter- and size-specific
527 patterns of fish seasonal migration between a shallow lake and its streams. *Ecol. Freshw. Fish* 17, 406–
528 415. <https://doi.org/10.1111/j.1600-0633.2008.00291.x>
- 529 Sleeter, T.D., Coull, B.C., 1973. Invertebrates associated with the marine wood boring isopod, *Limnoria*
530 *tripunctata*. *Oecologia* 13, 97–102. <https://doi.org/10.1007/BF00379623>
- 531 Trambly, Y., Somot, S., 2018. Future evolution of extreme precipitation in the Mediterranean. *Clim.*
532 *Change* 151, 289–302. <https://doi.org/10.1007/s10584-018-2300-5>
- 533 Wohl, E., Lane, S.N., Wilcox, A.C., 2015. The science and practice of river restoration: THE SCIENCE
534 AND PRACTICE OF RIVER RESTORATION. *Water Resour. Res.* 51, 5974–5997.
535 <https://doi.org/10.1002/2014WR016874>
- 536 Zeng, N., 2008. Carbon sequestration via wood burial. *Carbon Balance Manag.* 3, 1.
537 <https://doi.org/10.1186/1750-0680-3-1>
- 538 Zittis, G., Hadjinicolaou, P., Klangidou, M., Proestos, Y., Lelieveld, J., 2019. A multi-model, multi-
539 scenario, and multi-domain analysis of regional climate projections for the Mediterranean. *Reg.*
540 *Environ. Change* 19, 2621–2635. <https://doi.org/10.1007/s10113-019-01565-w>
- 541

542 **Plate & Figure captions:**

543 Plate I: RFID System. The detection system is mounted on a carrying rack to traverse the river in search
544 of tagged badges; RFID tags are inserted inside the pieces of wood. When a tag is detected, the reading
545 system displays the tag's identification code, the signal reception strength indication (RSSI), and the
546 geographic coordinates of the detection point on a liquid crystal display. All information is stored on a
547 micro SD card.

548 Plate II: After the initial movement, the RFID tagged wood pieces assumed a more natural position than
549 when initially introduced into the riverbed. Wood logs are found in large logjams, wedged between
550 rocks, beneath large logs, or simply deposited directly on the riverbed.

551 Figure 1: Study Site – Location and course of the Massane River. The polygon delineates the boundaries
552 of the National Nature Reserve of the Massane Forest.

553 Figure 2: Deadwood in the upper river riparian forest - (A) Mapping of the locations of large wood pieces
554 along the riverbed within the boundaries of the Massane Forest National Nature Reserve; (B) Boxplots
555 of length and volume distributions of individual wood pieces.

556 Figure 3: RFID-tagged wood logs. (A) Example of received signal strength indication (RSSI) levels vs.
557 distance between RFID tag and reader system. Each point represents an individual measurement; solid
558 points indicate values used for free space path loss (FSPL) signal model calibration. (B) RSSI_0 levels,
559 signal attenuation parameters (n), and maximum detection distance of RFID tags in field conditions.

560 Figure 4: RFID-tagged wood log locations. (A) Pre-flood, (B) Post-flood event. The polygon outlines the
561 boundaries of the National Nature Reserve of the Massane Forest.

562 Figure 5: Barplot of RFID-tagged wood log travel distances. The x-axis labels indicate the initial tag
563 positions relative to each other, from the source of the river to the exit of the river from the Reserve.
564 Color and color tone of the bars represent whether a log was located inside (blue) or outside (green)
565 the watercourse and its context, whether isolated (light tone) or aggregated within a logjam (dark tone)
566 after displacement.

567

568

569 Plate I

570



571

572 Plate II

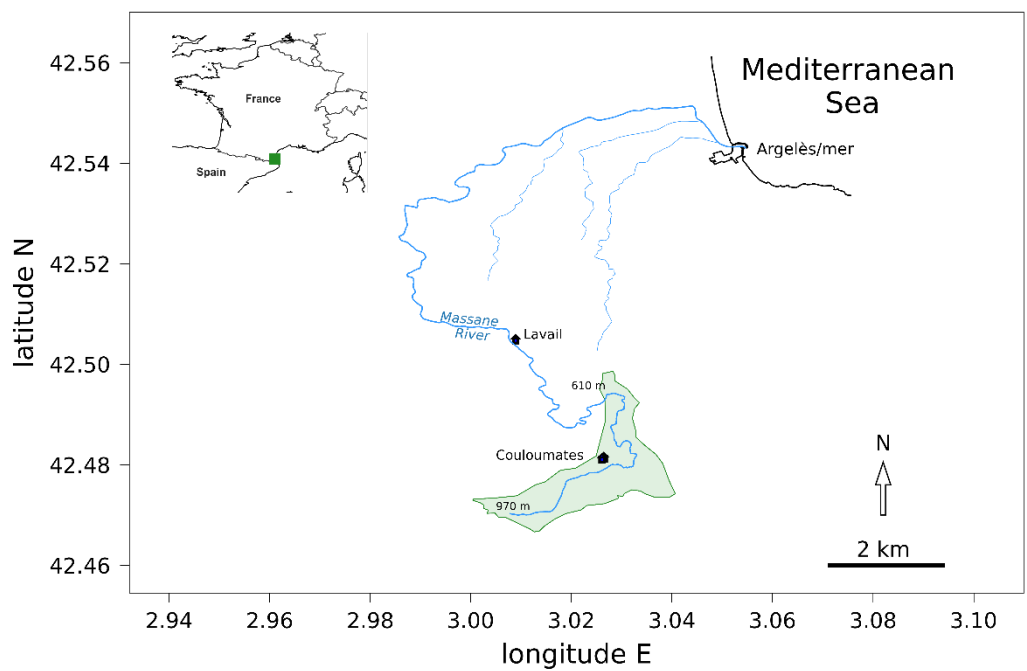
573



574

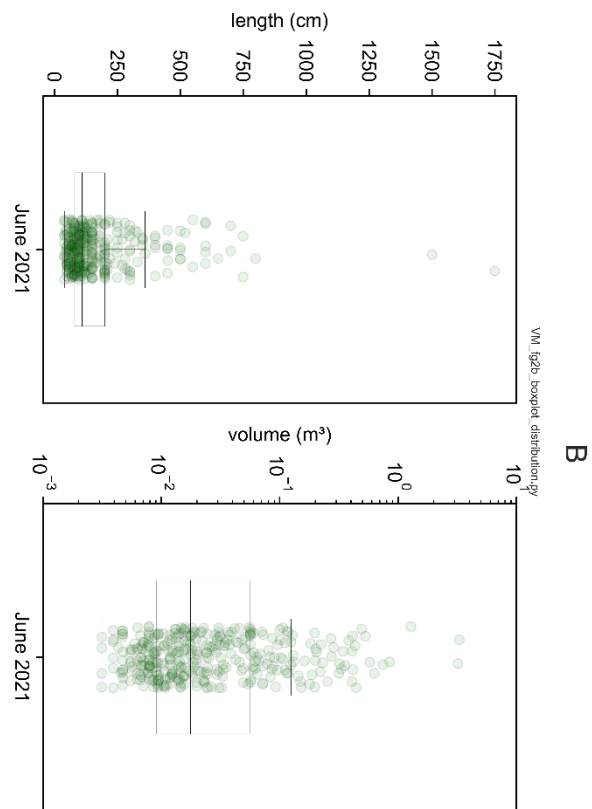
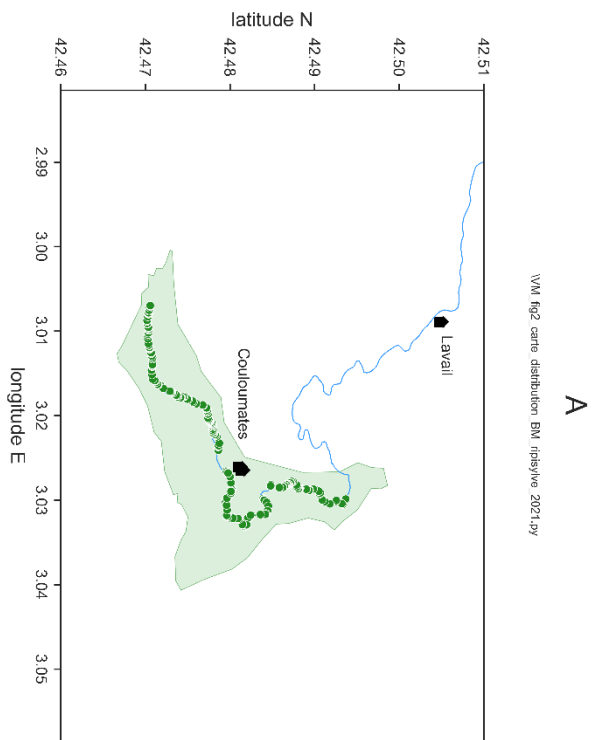
575 Figure 1

D:\Documents\Massane\Bois_Mort_Ripisylve\VM_fig1_fond_de_carte.py

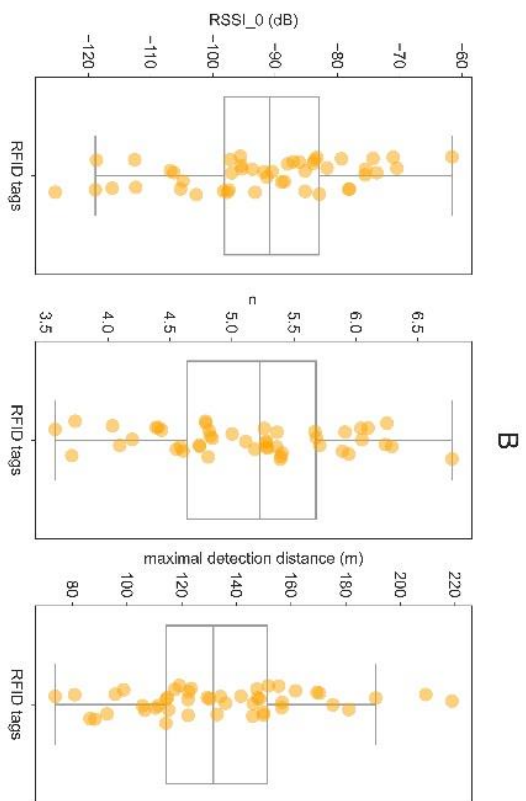
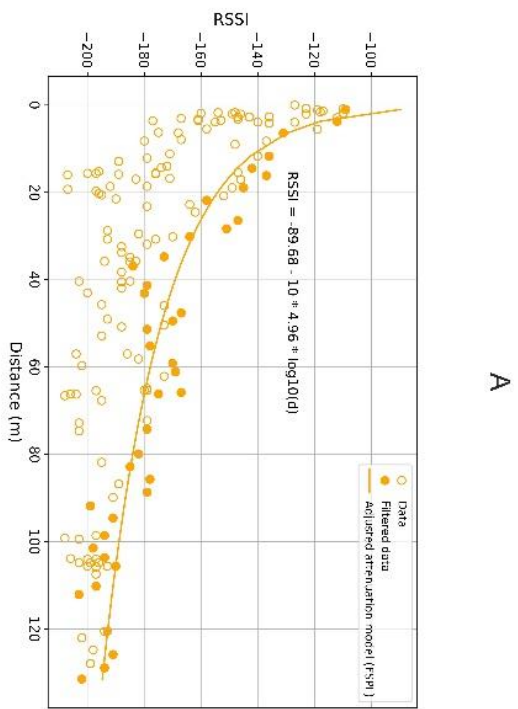


576

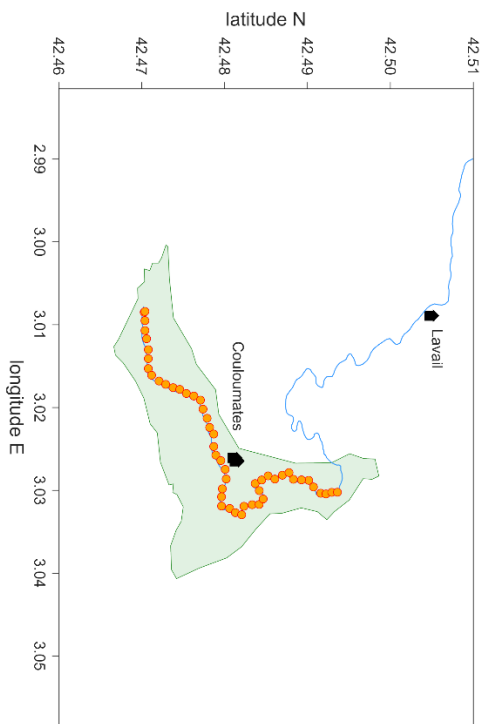
577 Figure 2



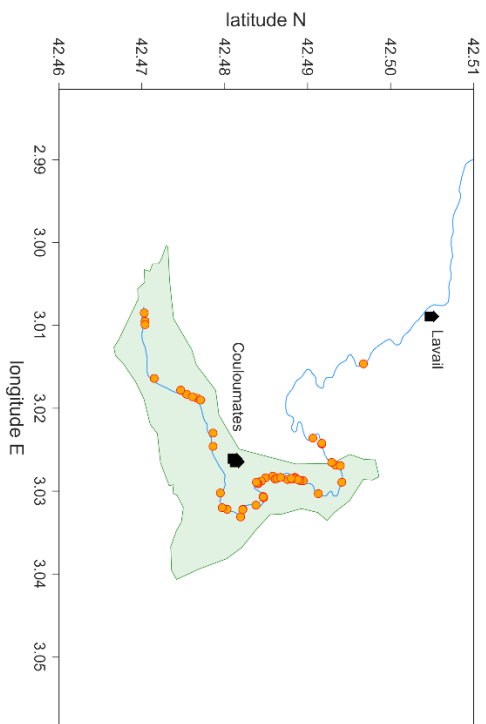
579 Figure 3



581 Figure 4



A



B

583 Figure 5

